© Institute of Materials Engineering Australasia Ltd

Extrusion of AlMgSi Alloys

O. Reiso

Hydro Aluminium R&D, Pb 219, N-6601 Sunndalsøra, Norway

Keywords: Extrusion, productivity, properties, AlMgSi-alloys, homogenisation, billet preheating.

Abstract

The present paper outlines the important role of the extrusion process in the aluminium industry and discusses the effect of some key factors that determine productivity and product properties during extrusion of AlMgSi alloys. The effects of alloy chemistry, homogenisation practice and billet preheating practice are described. The observed effects are explained in terms of the microstructure evolution of the material, in particular the effect of the distribution of the main alloying elements Mg and Si.

1. Introduction

Extrusion of aluminium alloys offers a relatively cheap method of producing complex shapes in long lengths with high geometric tolerances. The flexibility of the process with respect both to the alloys that can be extruded as well as the shapes possible to make has resulted in a widespread use of aluminium extrusions in today's everyday life. Aluminium extrusions are used in areas such as the building industry (window and door frames, building structures, roofing, curtain walling, etc.), shipping and offshore industry, furniture, and in the transportation sector for aerospace applications, rail vehicles and automotive applications.

Figure1 shows the aluminium consumption in Western Europe in year 2001 (approximately 8 million tonnes) split on the different product types [1]. As can be seen close to one third of the consumption is extruded products. The amounts of the different alloys used for extrusion purposes are shown in Figure 2 [2]. Clearly the dominating alloy system for extrusion of aluminium is the 6000 alloy system, i.e. AlMgSi alloys. More than 90% of the total extruded volume is estimated to be made from this alloy system.

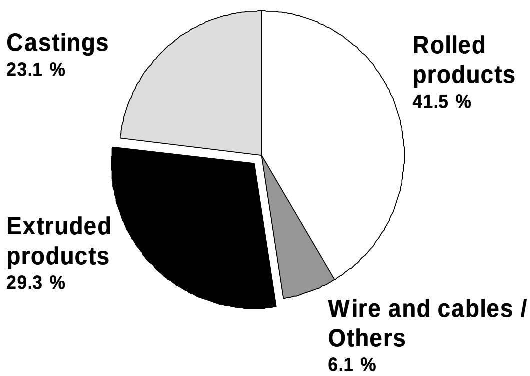

Figure 1: The aluminium consumption in Western Europe in 2001 split on the different product groups.

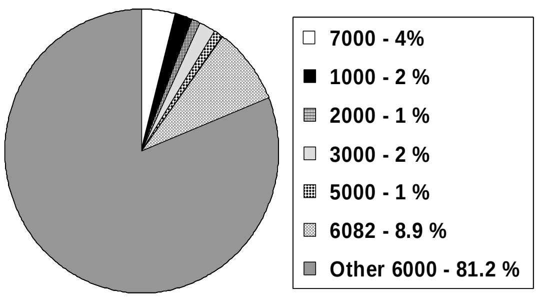

Figure 2: Aluminium alloys used for extrusion purposes. Western Europe, 2000.

The reason for this is that the alloys offer an attractive combination of properties such as mechanical properties, high corrosion resistance, high extrudability and formability as well as a good surface appearance and a good response to surface decorative and protective processes such as anodising and lacquering.

The main market for extruded products is within the building sector with a consumption of approximately 50% of the extruded volume in Western Europe in year 2001, Figure 3 [1]. However, due to its light weight and attractive properties aluminium extrusions are extensively used also in the transportation sector. Especially automotive applications have been focused by the industry, due to the high metal volumes involved. This sector is very challenging and contributes strongly to set the framework for further developments in aluminium alloy technologies.

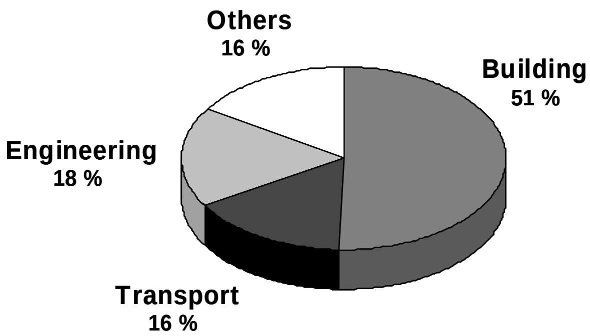

Figure 3: Markets for extruded products in Western Europe, 2001 [1].

When it comes to the applicability of aluminium extrusions in the automotive sector two focused areas are material price and properties. Thus productivity as well as correct and consistent mechanical properties become very important factors. Performance of the end product (life time, crash worthiness, etc.) is important, but also consistent properties in forming and fabricating operations during manufacturing are important in order to bring the production cost down. Also, a major advantage of using aluminium components is the ease by which aluminium can be recycled into new products without deteriorating its properties.

In the following some important factors in the production of aluminium extrusions will be illustrated by focusing on the effect of alloy chemistry and some important process parameters on extrudability (productivity at the press) and their effect on the mechanical properties of the extruded material. Other properties such as corrosion, response to surface treatment, weldability and machinability are also affected by the process parameters but will not be discussed here. Because of their dominating role only extrusion of AlMgSi alloys will be discussed.

2. Process Steps in the Production of Extrusions

Figure 4 shows a sketch of the different process steps in the production of aluminium extrusions. Melt treatment and alloying, DC casting of extrusion ingots and homogenisation of the ingots are all done in the casthouse. Then the ingots are shipped to the extrusion plants where they are first preheated to the desired extrusion temperature, extruded, cooled, stretched and aged. Figure 5 shows the temperature and time-course through the same process steps with indications of typical temperatures and times used during extrusion of AlMgSi alloys. Note that the time scale varies a lot for the different steps and also note the high heating rate encountered during the extrusion operation.

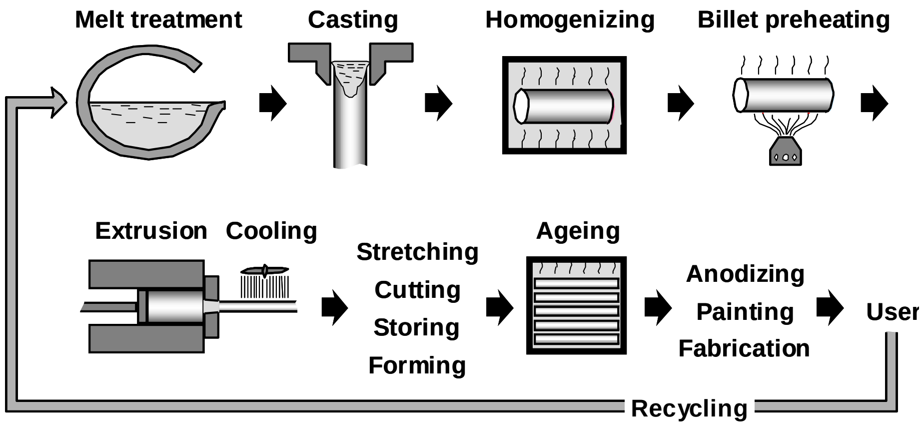

Figure 4: Sketch of the different process steps related to the production of extrusions.

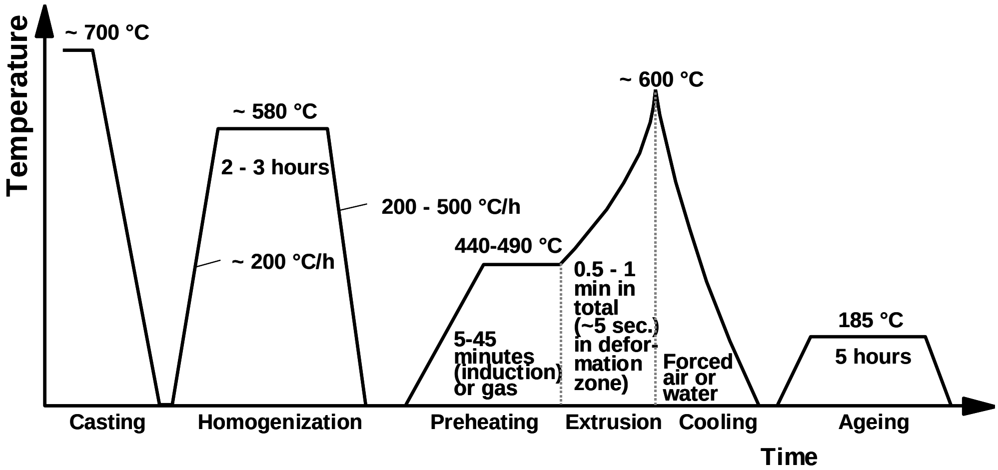

Figure 5: Sketch of the temperature/time profile for the production of extrusions. Typical temperatures and times used for AlMgSi alloys are indicated.

3. Limitations of Extrusion Speed

The productivity in an extrusion plant may be limited from numerous reasons. Considering the press itself, the extrusion speed may be limited by factors such as available pressure, unbalanced metal flow (for example different speeds of extrusions in a multiple hole die), geometric tolerances and the occurrence of defects in the surface of the extruded section. From a metallurgical point of view it is especially the limitations from the occurrence of the surface defects that are of main interest.

Examples of such surface defects may be die lines (shallow grooves in the surface parallel to the extrusion direction), pick-ups (small scars in the surface), tearing or hot shortness (surface cracks) and spalling (local thinning of the cross section). There may be many reasons for these speed limiting surface defects. One important reason (especially for tearing, hot shortness and spalling) is the onset of local melting reactions in the material during extrusion.

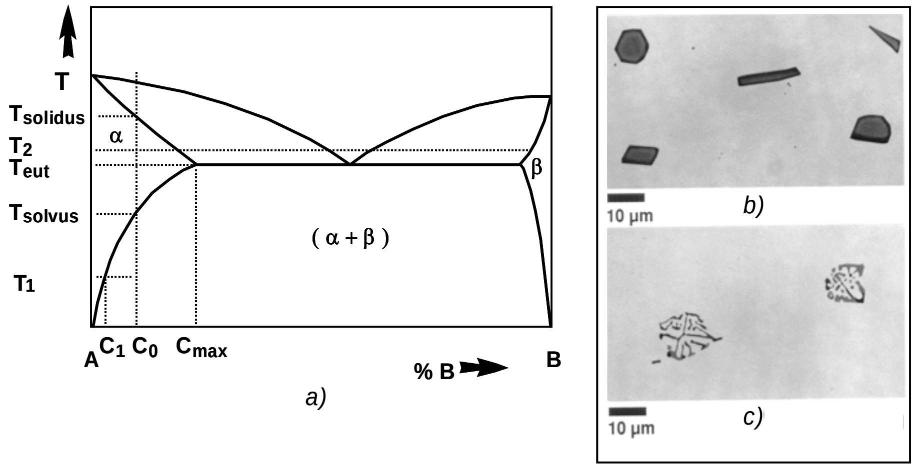

Figure 6: Internal melting in eutectic alloy systems. (a) A schematic eutectic binary phase diagram. (b) Mg_2Si particles in an Al-0.57wt%Mg-0.33wt%Si alloy after slow cooling from the homogenisation temperature and (c) eutectic (Al-Mg_2Si) microstructures formed during up-quenching of the structure in Figure6b to 600°C in a salt bath (no holding time) followed by quenching in air.

Figure 6 shows an example of such a melting reaction of secondary Mg_2Si particles together with their surrounding Al matrix. Consider an alloy of composition C_0 in a binary eutectic alloy system (Figure 6a) that has first been homogenised and then heat-treated at a temperature T_1 in order to precipitate β-phase particles. Upon slow heating of the alloy these β-phase particles will start to dissolve in the Al matrix and at or slightly above the solvus temperature for this particular alloy these particles will be completely dissolved. Upon further heating the alloy will start to melt as its solidus temperature is reached. If, however, the alloy is heated at a higher rate from the low temperature T_1 the precipitated β-phase particles will not have time enough to dissolve as the solvus temperature is reached and if they are still present as the eutectic temperature is reached or exceeded (T_{eut} or T_2 in Figure 6a) they will melt together with their surrounding Al matrix. In this situation melting of the material starts at a much lower temperature than in the case when the β-phase particles dissolve during heating. (T_{eut} versus $T_{solidus}$).

Figs. 6b and c show an example of a melting reaction in an AlMgSi alloy where large Mg_2Si particles have precipitated during slow cooling of the alloy from the homogenisation temperature (Figure 6b). Upon rapid heating of the alloy in a salt bath these Mg_2Si particles together with their surrounding matrix melts as the eutectic temperature is exceeded. If the sample is redrawn from the salt bath before the Mg and Si in the liquid diffuse into the Al matrix the melt will form a eutectic structure in the subsequent solidification reaction, as shown in Figure 6c.

The reaction rates for such local melting reactions have been found to be very high [3,4] and may thus take place also during the very high heating rates encountered during the extrusion operation. (Figure 5).

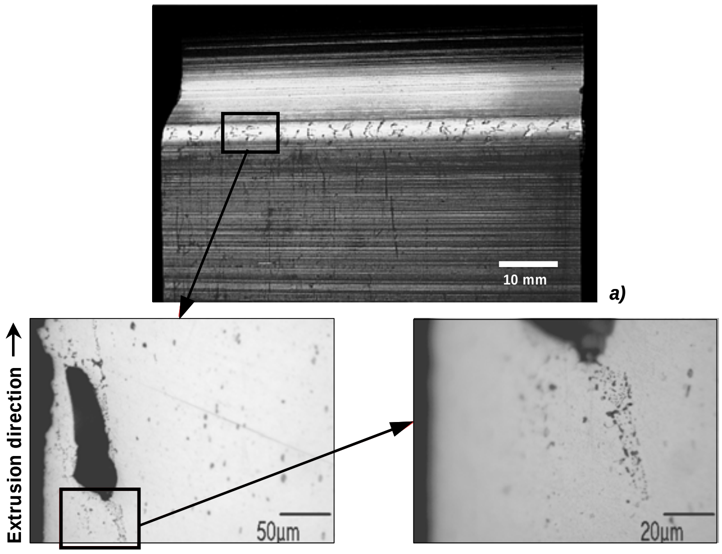

Figure 7: Surface tearing in an extruded section of a 6082 alloy Figure7a) and eutectic Al-Mg_2Si microstructures in a metallographic sample from a cross section through the tearing area, Figs. 7b) and c).

Figure 7 shows an example of tearing in the surface of an extrusion made from an AA6082 alloy (AlMgSiMn). The extrusion ingot contained large Mg_2Si phase particles and large Al-Mg_2Si eutectic volumes of the same type as shown in Figure 6c can be recognized in the tip of the tearing (Figure 7c), indicating that tearing was caused by this local melting reaction during extrusion.

4. The Effect of Alloy Composition

Figure 8 shows the effect of the main alloying elements Mg and Si on the maximum extrusion speed before tearing occurs in the surface of the extrusion. The two curves in each of the figures are from two different extrusion tests [5]. The absolute values of the maximum extrusion speeds in each of these tests are therefore not directly comparable, but the slopes of the curves have approximately equal values from both extrusion tests.

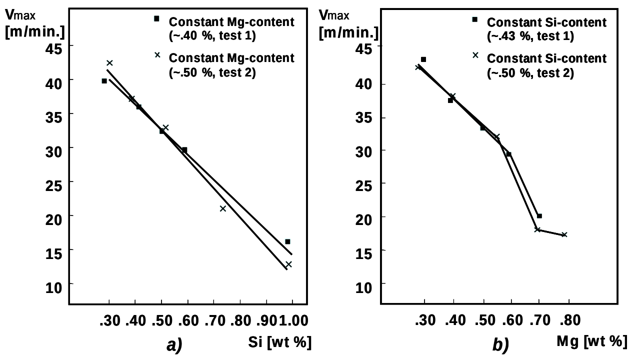

Figure 8: Maximum extrusion speed vs. Si content for two approximately constant levels of Mg (Figure8a) and vs. Mg content for two approximately constant levels of Si (Figure8b).

As shown in the figure the extrudability of the 6xxx series alloys is strongly affected by their alloy compositions. From Figure 8a it can be seen that the extrudability is reduced by 1-2% per 0.01wt% increase in the Si content of the alloy. The same strong effect is also observed from variations in the Mg content up to approximately 0.55wt% Mg (Figure 8b).

Above this concentration the effect of an increased Mg content is even more detrimental to the extrudability.

The reason for the observed variation in extrudability has been attributed to the change in the microstructure of the material with increasing alloy compositions. First, consider the alloys with relatively low contents of Mg and Si. For the applied set of process parameters (such as homogenisation practice and billet preheating practice) all the Mg and Si content of these alloys is in solid solution during extrusion, and the tearing on the surface is observed at profile exit temperatures close to the solidus temperatures of the alloys [6]. The Mg and Si contents determine the solidus temperature of the alloys, but they also have an impact on the deformation resistance, and thus the heat generation, during extrusion. The solidus temperature decreases and the deformation resistance increases with increasing Mg and Si contents. The solidus temperature is more sensitive to the Si concentration [7], while the deformation resistance is more sensitive to the Mg concentration [8]. It turns out that the resulting effect of Mg and Si in solid solution on the maximum extrusion speed before tearing is approximately equally strong, as shown in Figure8.

Secondly, for the given set of process parameters and at higher alloy compositions, Mg and Si will start to precipitate as Mg_2Si particles in the material before it is extruded. As a consequence the extrudability will be even further reduced due to the onset of melting in the material at a lower temperature (i.e. the eutectic temperature) than if the material contains no such Mg_2Si particles (see Figs. 6 and 7). This explains the sudden drop in extrudability at the higher Mg contents, as observed in Figure 8b.

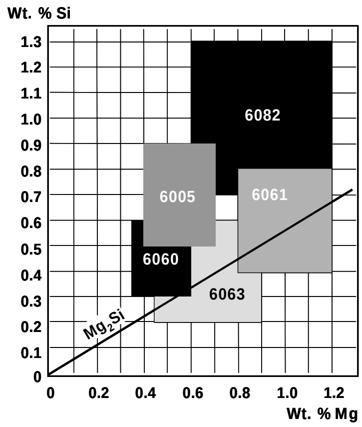

Figure 9: The most commonly used AlMgSi alloys for extrusion purposes. (Only Mg and Si content shown here).

The selection of the appropriate alloy to be extruded is done in order to meet certain requirements of the end product. In general the strength of the extruded sections increase with increasing amounts of Mg and Si in the alloys. If the extruded product is to meet a specific minimum strength requirement, this requirement can be met by the use of several alloys. However, from Figure 8 it can be seen that it is very important to select alloy compositions that do not overshoot the strength requirement of the end product to any large extent, because this will significantly reduce the productivity at the extrusion press.

The most commonly used 6xxx alloys for extrusion purposes are shown in Figure 9.

Also in this figure is indicated a line along which the atomic ratio between Mg and Si in the alloys is 2:1. It is interesting to notice that most of the alloys used are actually on the Si side of this Mg_2Si line. The hardening phase in these alloys has until recently been believed to have the same Mg:Si ratio as the equilibrium Mg_2Si phase (i.e. 2:1). However, recent publications [9,10] have shown that the likely composition of the most effective hardening precipitates in this alloy system has a Mg:Si ratio closer to 1:1 which may explain why most of the selected 6xxx alloys for extrusion purposes are located on the Si side of the Mg_2Si line in Figure 9.

5. The Effect of Billet Preheating Practice

The effect of billet preheating temperature on maximum extrusion speed can be presented in the form of an extrusion limit diagram (for a given press, alloy and extrusion die) [11]. Figure 10 shows an example of such a diagram. The extrusion speeds at low billet temperatures are limited by the available pressure of the press because of the high deformation resistance at low billet temperatures. At higher billet temperatures the maximum extrusion speed decreases by increasing billet temperatures due to limitations in the quality of the extruded sections (e.g. surface quality). Thus there apparently exists an optimum billet preheating temperature in order to maximise the extrusion speed. However, there are several reasons why a higher billet temperature than this optimum billet temperature is used, for example a requirement of minimum and/or consistent mechanical properties. (See below).

Figure 11 represents the right hand side of such an extrusion limit diagram and shows some results from an industrial extrusion test where the maximum extrusion speed before tearing occurs has been plotted vs. the billet temperature before extrusion [12]. It was found that when the billets were heated directly to the desired temperature, the maximum extrusion speed decreases with increasing billet temperature. At a billet temperature of approximately 500˚C the curve is shifted upwards to higher extrusion speeds before the speed again decreases with increasing billet temperatures.

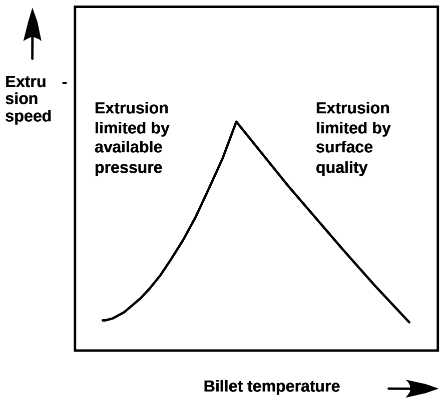

Figure 10: Sketch of an extrusion limit diagram.

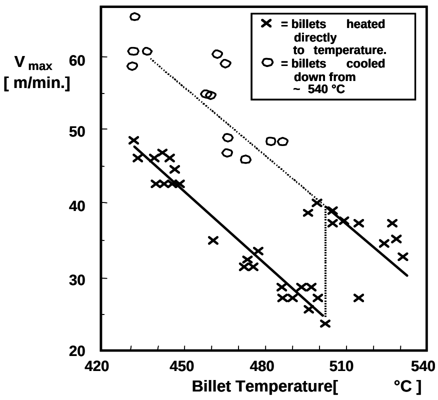

Figure 11: Maximum extrusion speed before tearing occurs vs. billet temperature. Solid line: directly heated billets. Dashed line overheated billets. Alloy: Al-0.60wt%Mg-0.48wt%Si-0.20wt%Fe.

The reason for this is to be found in the microstructure of the material. For this specific alloy large Mg_2Si phase particles exist in the material at low billet temperatures. As shown in Figs. 6 and 7, internal melting in the material may take place when the eutectic temperature is exceeded during extrusion and initiate surface tearing in the section [6]. However, at a high enough preheating temperature these Mg_2Si phase particles will dissolve and the eutectic temperature may be exceeded during extrusion without the occurrence of any melting reactions. (The solvus temperature of this alloy is close to

500˚C [7]). As shown in Figure 6 melting will now occur at a temperature close to the solidus temperature. This higher critical temperature for tearing initiation allows for more heat to be generated, which again allows a higher extrusion speed before tearing occurs. This is seen by the upward shift in the extrusion speeds for high billet temperatures in Figure 11.

Figure 11 also shows the maximum extrusion speed before tearing for some billets that were overheated prior to extrusion, i.e. the billets were first preheated to a temperature of 540˚C in order to dissolve the Mg_2Si particles and subsequently cooled down to the indicated temperatures before extrusion (Figure11, circle symbols). As can be seen, for this specific extrusion die these overheated billets could be extruded at significantly higher speeds than billets heated directly to the same temperatures. Even in this case the explanation can be related to changes in the microstructure. The overheated billets were cooled down to temperatures below the Mg_2Si solvus temperature quick enough to avoid any new precipitation of Mg_2Si particles before they were extruded. In this way the critical temperature for tearing initiation is higher in these billets as compared to the directly heated billets and the overheated billets could consequently be extruded faster in this case [6].

Table 1 shows a grading of the surface quality after visual inspection with respect to the amount of pick-ups in the surface of the extrusion from the same test as shown in Figure 11 as well as the number density of large Mg_2Si phase particles found in the same extrusions. As can be seen there is a strong relation between the number of Mg_2Si particles and the amount of pick-up, thus strongly indicating the melting reaction of Mg_2Si particles and their surrounding aluminium matrix to be one of the reasons for pick-up formation.

Table 1: Number of Mg_2Si phase particles of diameter > 1 µm within an area of 0.51 mm^2 in extrusion samples from different billet temperatures and a grading of the extrusion surface quality with regard to the amount of pick up.

	Billets heated directly to temperature								Billets cooled down from ~ 540 °C		
Billet temp.[°C]	432	442	446	477	488	506	511	527	466	466	430
No. of particles	1559	1514	446	122	131	8	5	3	38	5	19
Pick up grading	III	III	II	II	II	I	I	I	I	I	I

Coarse Mg_2Si phase particles do not contribute to the strengthening of these alloys. Thus, if the extrusions contain such particles, the Mg and Si content tied up in these particles will not be available to form hardening particles during the subsequent ageing procedure. Due to the dissolution of coarse Mg_2Si particles, the strength of extruded sections from billets that contain such particles will increase by increasing billet temperatures for billets heated directly to the extrusion temperature. In Figure 12 this is shown to be the case for aged extrusions from a 6060/6063 type of alloy. At billet temperatures above approximately 470˚C the ultimate tensile strength is levelling out and also the spread in the strength values is reduced.

This level represents the maximum strength potential for this alloy and ageing procedure all the Mg- and Si-atoms in the alloy are in solid solution in the extruded section and thus available for precipitation of the hardening particles during artificial ageing.

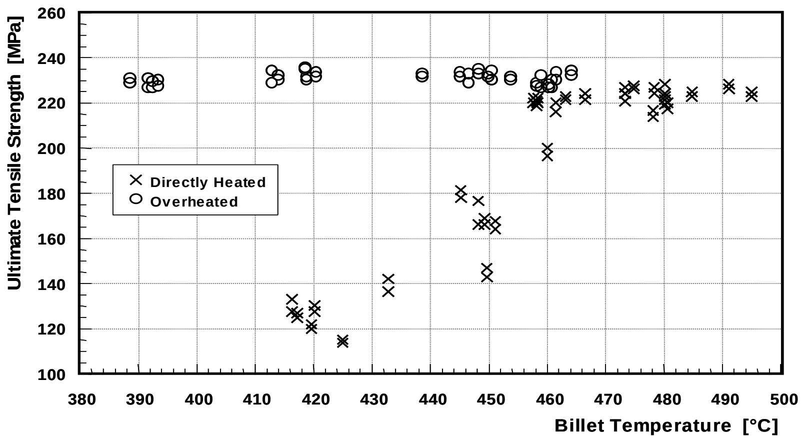

Figure 12: The effect of billet preheating practice on the ultimate tensile strength in aged extrusions. Alloy composition: Al-0.51wt%Mg-0.42wt%Si-0.20wt%Fe.

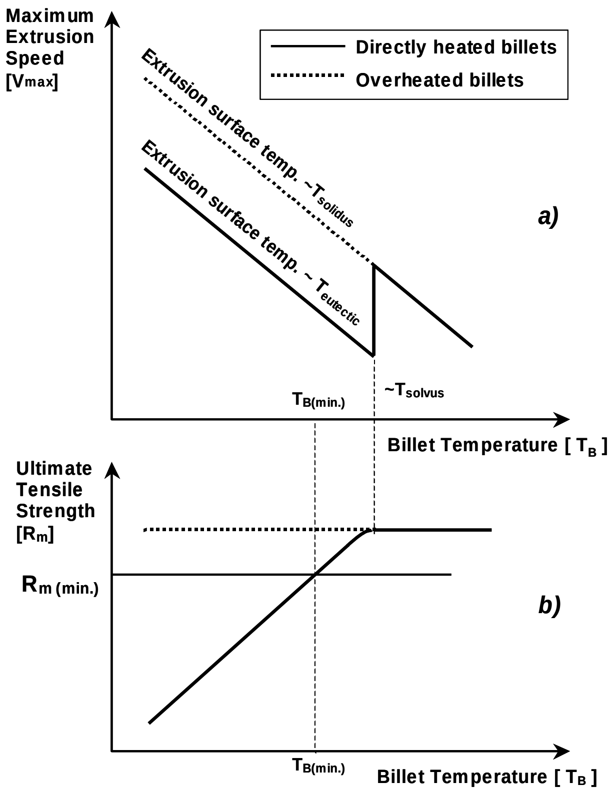

Figure 13: Maximum extrusion speed (a) and ultimate tensile strength in aged extrusions (b) vs. billet temperature. $R_{m(min)}$ represents a minimum strength requirement in the product and $T_{B\ min}$ the minimum billet temperature for directly heated billets in order to achieve this requirement.

Figure 12 also shows the strength values for aged extrusions from billets that were first overheated and cooled down to the indicated billet temperatures before extrusion.

As already argued these extrusions contain all of the Mg- and Si-atoms in the alloy in solid solution after extrusion and thus show the maximum strength value for this alloy regardless of billet temperature. As can be seen, consistency in mechanical properties is also found to be very high for these extrusions.

The effect of the billet temperature on the maximum extrusion speed and on the strength of the aged sections is summarised in Figure 13. A minimum strength requirement for a given section is indicated by $R_{m(min)}$ (Figure 13b). In order to achieve this strength requirement the billet temperature has to exceed a certain minimum value, $T_{B\ (min)}$, for directly heated billets. As can be seen from Figure 13a this demand of a billet temperature above $T_{B\ (min)}$ results in low extrusion speeds and thus reduced press productivity.

If, however, overheating is applied there are no restrictions on the billet temperature with respect to mechanical properties of the sections. As a result lower billet temperatures may be applied (utilising the maximum force of the press) and thereby significant increases in the extrusion speed may be obtained. (Also critical temperatures for tearing initiation have been indicated in the figure as well as the "location" of the solvus temperature for the applied processing conditions).

These results clearly illustrate the importance of a strict control of the billet temperature during extrusion, both from a product quality as well as a productivity point of view.

6. The Effect of Homogenisation Practice

The heating rate to the homogenisation temperature, the homogenisation temperature and time as well as the cooling rate from the homogenisation temperature may all influence extrudability and section properties. In the present presentation only the effect of the cooling rate from the homogenisation temperature will be discussed.

Figures 14-16 show the effect of the cooling rate after homogenisation on the maximum extrusion speed, the breakthrough pressure and the tensile strength of the extruded sections for a 6060/6063 type of alloy [13].

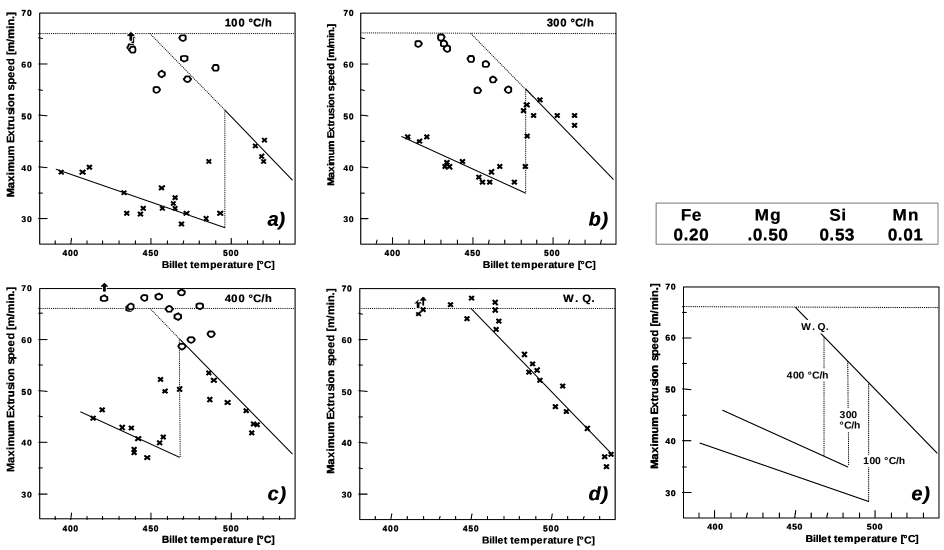

Figure 14: Maximum extrusion speed vs. billet preheating temperature for different cooling rates after homogenisation: 100°C/h (a), 300°C/h (b), 400°C/h (c) and water quenching (W.Q.) (d). x = billets heated directly to temperature, o = billets cooled down from ~ 540°C. Figure (e) shows the results from the directly heated billets in the same graph.

Four different cooling rates were selected: 100°C/h, 300°C/h, 400°C/h and water quenching (estimated to approximately 50000°C/h). Figures. 14 a-d show how the maximum extrusion speed is influenced by the billet preheating temperature for each of these cooling rates from the homogenising temperature for directly heated billets as well as for overheated billets. (The same type of curves as previously presented in Figure 11). In Figure 14e the curves from Figures. 14 a-d are shown together for comparison. As can be seen from Figure 14e, the transition temperature from where the maximum extrusion speed is limited by internal melting of Mg_2Si particles and the surrounding Al matrix to where the extrudability is limited by solidus melting in the material (Figure 13a) is shifted towards lower billet preheating temperatures by increasing cooling rates after homogenisation.

The water quenched billets show no such transition in maximum extrusion speed, i.e. they could all be extruded at the same high speeds as the overheated billets (see Figure 14 a-c).

The extrudability is thus significantly increased by an increasing cooling rate after homogenisation. This is can be explained by reference to changes in the microstructure. At low cooling rates from the homogenisation temperature the material contains large Mg_2Si phase particles which will cause melting to occur at low temperatures during extrusion. These particles will need extensive time to dissolve during preheating, i.e. with a given preheating time of the billet these particles need a high preheating temperature before they dissolve. By increasing cooling rates the size of these Mg_2Si particles is reduced. Thus, these smaller particles will dissolve at lower billet preheating temperatures and the shift in extrusion speed is consequently occurring at lower billet temperatures.

The water quenched billets were cooled at a rate high enough to avoid any precipitation of Mg_2Si particles. Also, the heating rate to the extrusion temperature in this particular case was high enough to avoid precipitation of harmful Mg_2Si particles during preheating. (An induction furnace was used). These billets could thus all be extruded at high speeds regardless of the variation in billet preheating temperature, i.e. with no shift to lower extrusion speeds at low preheating temperatures.

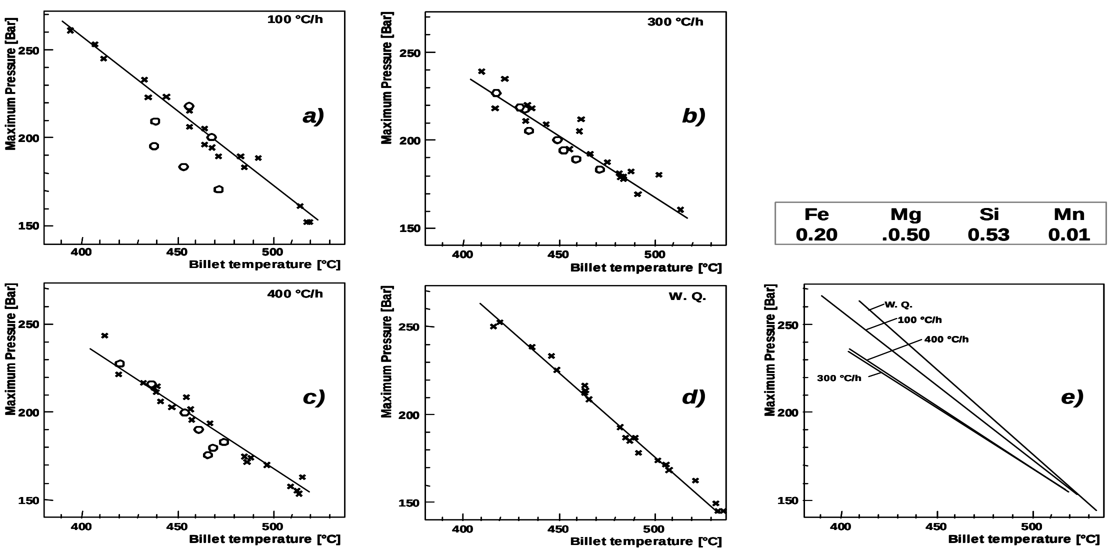

Figure 15: Maximum extrusion pressure vs. billet preheating temperature for different cooling rates after homogenisation: 100°C/h (a), 300°C/h (b), 400°C/h (c) and water quenching (W.Q.) (d). x = billets heated directly to temperature, o = billets cooled down from ~ 540°C. The results from the directly heated billets are shown in the same graph in figure (e).

Figure 15 shows the maximum extrusion pressure vs. billet preheating temperature for the different cooling rates after homogenisation. Figure 15e shows that the water quenched billets have the highest breakthrough pressure (i.e. the highest deformation resistance), especially at low billet temperatures. The curves are approaching the same values for high billet temperatures because the Mg_2Si particles dissolve in all variants at a high enough temperature. This results in the same amount of Mg- and Si-atoms in solid solution and thus the same deformation resistance in the different variants. In spite of the higher deformation resistance, the extrudability of the water quenched billets are better than the air cooled variants, especially at low billet temperatures. (The higher recordings of the breakthrough pressure for the cooling rate of 100C°/h as compared to the other air cooled variants help explain the lower extrusion speeds at low billet temperatures observed for this variant).

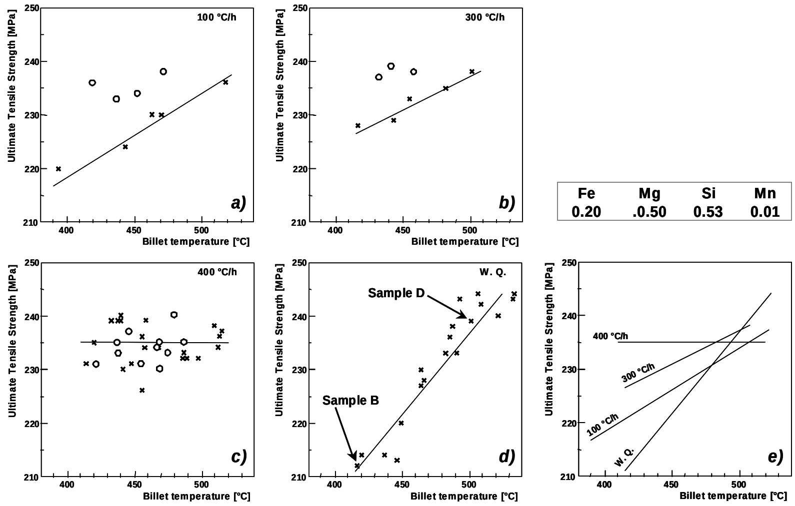

Figure 16: Ultimate tensile strength in the aged extrusions vs. billet pre-heating temperature for different cooling rates after homogenisation: 100°C/h (a), 300°C/h (b), 400°C/h (c) and water quenching (W.Q.) (d). x = billets heated directly to temperature, o = billets cooled down from ~ 540°C. The results from the directly heated billets are shown in the same graph in figure (e). Ageing practice: 185°C, 5 hours holding time.

Figure 16 shows the ultimate tensile strength vs. billet temperature of the aged extrusions for the different cooling rates after homogenisation. As expected, Figure 16e shows that the strength of the aged extrusions from the directly heated billets increases with increasing billet temperatures and also with increasing cooling rates after homogenisation for the air cooled billets. (At a cooling rate of 400C°/h from the homogenisation temperature the ultimate tensile strength shows a very little sensitivity to the billet temperature). Again this is due to the increasing amounts of Mg- and Si-atoms in solid solution after extrusion, thus increasing the amount of Mg- and Si-atoms available to form hardening particles during ageing of the alloy.

Very surprisingly, however, the strength of the extrusions from the water quenched billets were found to be very sensitive to the billet preheating temperature (Figure 16e). Because these billets contain no coarse Mg_2Si particles they were expected to show the highest strength values regardless of billet preheating temperature. The reason for this behaviour is shown in the TEM micrographs in Figure 17.

In spite of the very low supersaturation of Fe in aluminium, an investigation in a transmission electron microscope (TEM) revealed a very high number density of very small (10-30nm diameter) AlFeSi dispersoid particles in the extrusions from the water quenched billets. The number density of these dispersoid particles was found to decrease by increasing billet preheating temperatures [14]. The precipitation of these particles and the variation in their number density with billet temperature has been attributed to the nucleation conditions in the water quenched billets and a reduced supersaturation of Fe with increasing billet temperatures.

These AlFeSi dispersoid particles act as very good nucleation sites for β'-MgSi particles which may precipitate during cooling of the sections after extrusion. Forced air cooling of the section was used in this extrusion test, but in spite of the relatively high cooling rates obtained, severe precipitation of β'-MgSi particles has taken place in the extrusions from the water quenched billets. These β'-MgSi particles do not contribute to the strength of the material and if present they reduce the available amount of Mg- and Si-atoms to form hardening particles and consequently they reduce the strength after ageing. Because these β'-MgSi particles nucleate on the AlFeSi dispersoid particles, the amount of β'-MgSi increases with the number density of AlFeSi particles. Thus, the tensile strength is low for low billet preheating temperatures and increases with increasing billet preheating temperature for the extrusions from the billets that were water quenched after homogenisation. (No such small AlFeSi dispersoid particles were observed in the extrusions from the billets that were air cooled after homogenisation).

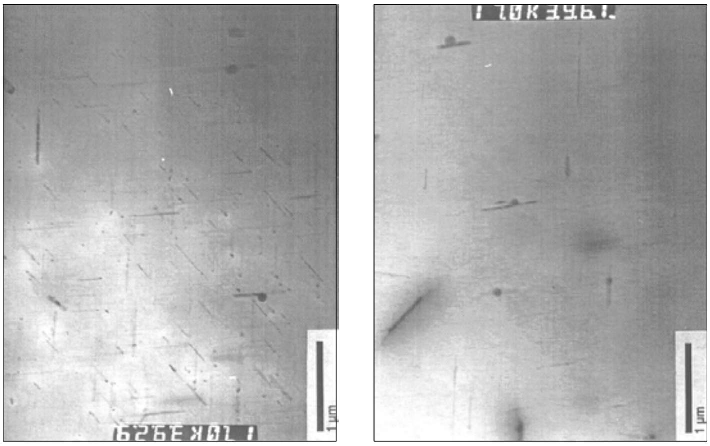

Sample B **Sample D**

Figure 17: TEM micrographs from extrusion samples from billets that were water quenched after homogenisation and preheated with a low (sample B) and a high (sample D) temperature [12]. (The samples are indicated on Figure 16 d).

If the extrusions had been cooled at a higher rate after extrusion (for example water quenched), high tensile strength values are to be expected also in the extrusions from the water quenched billets, regardless of billet preheating temperature. Thus the observed variation in tensile strength for the water quenched billets is a result of the variation in the quench sensitivity of the material.

Because of the challenges regarding water quenching of the extruded sections (distortion, water staining, etc.) air cooling of the sections is preferred. Consequently a conclusion to this discussion is that a high cooling rate with forced air from the homogenisation temperature is recommended.

The effect of the process parameters discussed may partly be summarised in the form of a modified extrusion limit diagram, shown in Figure 18. This diagram shows how the maximum extrusion speed varies with the billet temperature and how the transition temperature between the two modes of tearing initiation (i.e. eutectic melting and melting at or close to the solidus temperature) is affected by the alloy composition and the cooling rate after homogenisation.

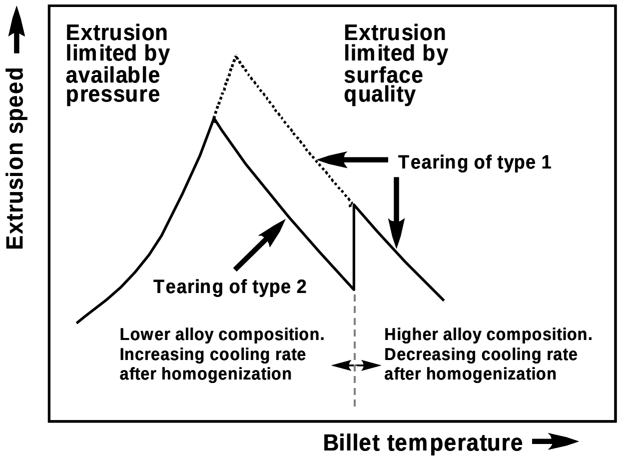

Figure 18: Modified extrusion limit diagram indicating how the transition temperature between the two modes of tearing initiation (i.e. eutectic melting, type 1, and melting at or close to the solidus temperature, type 2) is influenced by alloy composition and cooling rate after homogenisation.

Conclusions

This paper has put emphasis on the important role of the extrusion process and in particular extrusion of AlMgSi alloys in the aluminium industry.

Local melting reactions in the material during extrusion are identified as a factor determining the productivity limit for AlMgSi alloys. The effects of alloy chemistry, billet preheating practice and homogenisation practice on productivity and product properties during extrusion of AlMgSi alloys have been discussed.

The observed effects are explained in terms of the microstructure evolution in the material, in particular the distribution of the main alloying elements Mg and Si. Thus an optimum microstructure is determined by factors such as alloy composition and the whole thermal and thermo-mechanical history of the material. This means that in order to optimise productivity and product properties the process chain from melt to finished extrusions must be considered as a whole, and that what occurs at one stage in the process chain is not independent of the other stages.

Acknowledgments

The author is grateful to Hydro Aluminium for permission to publish this work.

References

[1] http://www.eaa.net, 2004-01-28, (The European Aluminium Association).[2] Hydro Aluminium, Extrusion Ingot Business Unit.
[3] O. Reiso, H. G. Øverlie and N. Ryum, Metall. Trans. Volume 21A, June, 1990, pp. 1689-1695.
[4] O. Reiso, N. Ryum and J. Strid, Metall. Trans. Volume 24A, December, 1993, pp. 2629-2641.
[5] O. Reiso, Proc. 3rd Int. Aluminum Extrusion Technology Seminar, Atlanta, GA, Aluminum Association, 1984, Vol. 1, pp. 31-40.
[6] M. Lefstad and O. Reiso, Proc. 6th Int. Aluminum Extrusion Technology Seminar, Chicago, IL, Aluminum Assosiation, 1996, Vol. 1, pp. 11-21.

[7] H.W.L. Phillips, “Annotated Equilibrium Diagrams of some Aluminium Alloy Systems”, The Institute of Metals, 17 Belgrave Square, London S. W. I, 1959, pp. 65-71.
[8] A.F. Castle and G. Lang, Aluminium, Vol.53, 1977, pp. 535-539.
[9] G.A. Edwards, K. Stiller, G.L. Dunlop and M.J. Couper, Materials Science Forum Vols. 217-222 (1996) pp. 713-718.
[10] S.J. Andersen, H.W. Zandbergen, J. Jansen, C. Træholt, U. Tundal and O. Reiso, Acta. mater., Vol. 46, No. 9, pp. 3283-3298, 1998.
[11] K. Laue and H. Stenger, “Extrusion”, American Society for Metals, Metals Park, Ohio 44073, 1981, pp.34-38.
[12] O. Reiso, Proc. 4th Int. Aluminum Extrusion Technology Seminar, Chicago, IL, Aluminum Association, 1988, Vol. 2, pp. 287-295.
[13] O. Reiso, O. Sjøthun, U. Tundal and J.E. Hafsås, Proc. 6th Int. Aluminum Extrusion Technology Seminar, Chicago, IL, Aluminum Association, 1996, Vol. 1, pp. 1-10.
[14] O. Reiso, U. Tundal and S. Andersen, Proc. 6th Int. Aluminum Extrusion Technology Seminar, Chicago, IL, Aluminum Association, 1996, Vol. 1, pp. 141-147.